Acta Technica *62* (2017), No. 7A, 581–600

Numerical modeling research on layout dimension optimization of lock manifold system in the lock chamber

Xingxing Zhang[1], Guangxiang Xu[1], Mingdong Chen[1], Ming Chen[1], Jiao Wang[2]

Abstract. Quality of layout dimension of the lock manifold system in the lock chamber is directly related to hydraulic performance of the whole dispersive water conveyance system. Fluent computing platform of large-scale fluid mechanics is applied in this Thesis to establish a three-dimensional mathematical model for water conveyance system of ports at side of the long gallery at the bottom of the lock. Mooring force of a ship is prepared and computational procedures are carried out with the help of UDF functions, achieving secondary development of FLUENT software. After verification by physical modeling experiments, this value method of relatively higher computation accuracy is reasonable and flexible. At the same time, numerical modeling calculation is carried out on mooring force of the ship with the lock chamber equipped with different aspect ratio (λ) of fracture surface of different ports' throats and number of ports (δ), and flow characteristics, for which the optimal value taking interval λ of δ and are proposed and layout principles for the lock manifold system in the lock chamber are summarized. Results show that 0.5 and 2 are not suitable for λ, that value in 0.9-1.1 interval should be taken as far as possible for λ, which guarantees smaller mooring force of the ship and good berth condition, that the value as 2-2.2 times of the lock chamber's width is the optimal value for δ, which guarantees fully dispersion of outflow from ports, relatively good energy dissipation effects, even water flow in the lock chamber and stable mooring force, contributing to the ship safety.

Key words. Lock, Lock manifold system, Mooring force, Flow characteristics, Physical modeling, Numerical modeling.

[1]National Engineering Research Center for Inland Waterway Regulation, Chongqing Jiaotong University, Chongqing, China

[2]Nanjing Hydraulic Research Institute, Nanjing, China

1. Introduction

In the design of dispersive water conveyance system for the lock, though there are various layout types, multiple ports (pipes) on the gallery are used to connect the lock chamber, forming a channel for water flowing from and to the lock chamber, i.e. so-called the lock manifold system in the lock chamber. To ensure even outflow from each port during water convergence process of the lock and reduce force of water flow from the lock on the ship, layout dimension of the manifold system, which includes port spacing, port number, aspect ratio of fracture surface of the port throat, ratio of total area of the port throat's fracture surface vs. area of main gallery, layout type of fracture surface area of the port throat, etc., must be determined reasonably. Limited by complicate turbulent flow field of the lock, physical model tests and prototype observation are important means to study layout dimension of the lock manifold system. Since the beginning of the 1930s-1940s, many domestic and foreign research institutes have done a lot of researches on the local dispersive water conveyance, water conveyance from ports at the side of gate wall's galleries and water conveyance type of longitudinal gallery at the bottom of lock and so on [1-19].

It is easy to find that berthing conditions of the ship in lock is determined through analysis on hydraulic characteristics of fracture surface of port throats in the above research results on numerical simulation, so as to comment on the advantages and disadvantages of the layout dimension of composite pipes. However, magnitude of the ship's mooring force is the gold standard to directly quantify the berthing conditions, for which determination and calculation of ship mooring force is the indispensable key link as to comparison & selection of different layout dimension scheme for composite pipes in the lock chamber. Methods for research on ship mooring force in the lock chamber are mainly theoretical derivation, experimental determination and numerical simulation, where the theoretical derivation is the most common research means. Moreover, scholars from the former Soviet Union, France, Germany, China, Holland and other countries provided relevant provisions and calculation formula on longitudinal and horizontal mooring force of the ship. However, due to the limitations of the equation on use conditions, the model test method is widely used in practical engineering. For example, Professor Caccia Malinowski from the former Soviet Union invented dynamometers for determination of mooring force of the ship filling and emptying water in a concentrated way in the lock; Richard L. Stockstill described measurement methods for the ship's mooring force with physical model tests, meanwhile, he analyzed dimensionless form of the added mass and damping coefficients and took these coefficients as constants of the elastic modulus to estimate mooring force of the ship based on model tests of flow field in the lock chamber [20]. A large number of studies are also carried out by Nanjing Hydraulic Research Institute, China that has developed a full circle resistance dynamometer. Due to the fact that the physical model test is time-consuming and laborious, it is imperative to develop the numerical simulation program to quickly obtain the mooring force of the ship. In the course of ship filling and emptying, the interaction between ship and water is a typical problem of fluid structure interaction. R.J.de Jong et al.

researched the effect of hydrodynamism of surge on the ship in the lock chamber and motion response of the ship and developed calculation procedure of longitudinal force suffered by the ship in the lock chamber while the lateral force was not considered [21]. Luigi Natale et al. simulated rising and falling motion of the ship under the action of surge with the ship's single-degree-of-freedom dynamic model [22]. Li Xianfang simulated the process of the ship rising with rising of free water in the lock chamber by using CFD commercial software and the dynamic mesh model and derived out solution to cable stress, however, coupling relationship between the ship and water flow is not fully considered in the calculation process [23].

In conclusion, as for simple and complicate dispersive water convergence type of the lock, fruitful results have been obtained with regard to selection and design of layout dimension of lock manifold system in the lock chamber and facts about port spacing, arrangement types of fracture surface area of port threat, total area of fracture surface of port throats and others are listed in the standard, however, research on aspect ratio of facture surface of port throat and number of ports are insufficient [24]. In view of this, based on dynamic response of fluid-structure interaction, longitudinal and horizontal force of the ship and motion control equations are built in this Thesis, besides, with UDF functions in the FLUENT software and C language used, parallel computing procedures for the ship's mooring force are prepared to carry out secondary development on software, making possible quick acquisition of the ship's mooring force. At the same time, the three-dimensional mathematical model of water conveyance system of ports at side of long gallery at the bottom of the lock is established, for which RNG $k \sim \varepsilon$ turbulent flow equation is used with many typical aspect ratio of fracture surface of port throats and number of ports selected to calculate mooring force of the ship in the lock chamber and flow characteristics under different conditions, values of which are optimized to summarize layout principles of composite pipes in the lock chamber, providing technical reference for design of subsequent dispersive water conveyance types of the lock of similar types.

2. Mathematical model

2.1. Flow control equation

RNG $k \sim \varepsilon$ turbulence model which is derived based on renormalization group theory is used for simulation of three-dimensional unsteady force produced during water conveyance of the lock. The control equation for tensor form of incompressible unsteady flow is as follows:

$$\frac{\partial \rho}{\partial t} + \frac{\partial u_i}{\partial x_i} = 0\,. \tag{1}$$

Continuity equation: $\frac{\partial \rho}{\partial t} + \frac{\partial u_i}{\partial x_i} = 0$

Momentum equation:

$$\frac{\partial(\rho u_i)}{\partial t} + \frac{\partial(\rho u_i u_j)}{\partial x_j} = -\frac{\partial p}{\partial x_i} + \frac{\partial}{\partial x_j}\left[(\mu + \mu_i)\left(\frac{\partial u_i}{\partial x_j} + \frac{\partial u_j}{\partial x_i}\right)\right] + \rho g_i\,. \tag{2}$$

Transport equation for turbulent kinetic energy k:

$$\frac{\partial(\rho u_i)}{\partial t} + \frac{\partial(\rho k u_i)}{\partial x_i} = \frac{\partial}{\partial x_j}\left(\alpha_k \mu_{eff} \frac{\partial k}{\partial x_j}\right) + G_k - \rho\varepsilon\,. \tag{3}$$

Transport equation for turbulent kinetic energy dissipation ε:

$$\frac{\partial(\rho\varepsilon)}{\partial t} + \frac{\partial(\rho\varepsilon u_i)}{\partial x_i} = \frac{\partial}{\partial x_j}\left(\alpha_\varepsilon \mu_{eff} \frac{\partial k}{\partial x_j}\right) + \frac{C^*_{1\varepsilon}\varepsilon}{k} G_k - C_{2\varepsilon}\rho\frac{\varepsilon^2}{k}\,. \tag{4}$$

Where, ρ and p are weighted average density of volume fraction and pressure correction separately; μ is molecular viscosity coefficient of volume fraction through weighted average; μ_t is turbulent viscosity coefficient, which can be calculated by turbulent kinetic energy k and turbulent kinetic energy dissipation ε by using $\mu_t = \rho C_\mu \frac{k^2}{\varepsilon}$; μ_{eff} is the effective coefficient of viscosity with $\mu_{eff} = \mu + \mu_t$; G_k is turbulent kinetic energy generation item caused by the mean velocity gradient with $C^*_{1\varepsilon} = C_{1\varepsilon} - \frac{\eta(1-\eta/\eta_0)}{1+\beta\eta^3}$, $\eta = \frac{k}{\varepsilon}\sqrt{(2E_{ij}\cdot E_{ij})}$ and $E_{ij} = \frac{1}{2}(\frac{\partial u_i}{\partial x_j} + \frac{\partial u_j}{\partial x_i})$.

In the above tensor expressions, u_i is velocity component along x_i direction with $i, j = 1, 2, 3$. Constants in the universal model in the equation are $C_\mu = 0.0845$, $\alpha_k = \alpha_s = 1.39$, $C_{1\varepsilon} = 1.42$, $C_{2\varepsilon}1.68$, $\eta_0 = 4.377$ and $\beta = 0.012$ respectively.

2.2. Longitudinal and horizontal force of the ship and motion equation

As for research on the coupling effect between the ship and water, in the ideal case, motion on the free surface of the ship about six degrees of freedom, while only three degrees of freedom, namely, pitching, rolling and translation motion along the vertical direction remain for the ship docked in the lock chamber due to restriction by cable. In order to simplify the calculation, effects of pitching and rolling are neglected during construction of equation of forces acting on the ship, and the translational motion along the vertical direction is taken into account only. Fig. 1 and Fig. 2 are forces on the ship in the lock chamber in the horizontal direction and the vertical direction, where x axis is the direction of the center line of the lock (longitudinal direction of the lock), y axis is ship rising direction with increasing water level in the chamber (vertical direction of the lock chamber) and z axis is the direction for outflow of ports (horizontal direction of the lock chamber).

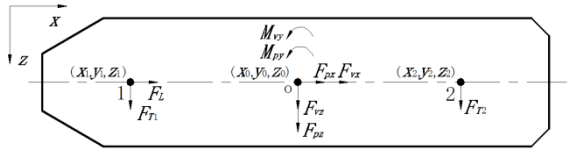

Fig. 1. Schematic diagram of forces on the ship in the horizontal direction

$$F_{px} = \int_{A_s} p_x dS, F_{pz} = \int_{A_s} p_z dS, F_{vx} = \int_{A_s} \tau_x dS, F_{vz} = \int_{A_s} \tau_z dS\,. \tag{5}$$

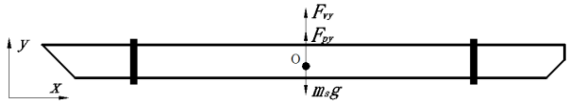

Fig. 2. Schematic diagram of forces on the ship in the longitudinal direction

$$M_{py} = M_o\left(F_{px}\right) + M_o\left(F_{pz}\right) = \int_{A_s} p_x(z - z_0)dS + \int_{A_s} p_z(x_0 - x)dS\,. \tag{6}$$

$$M_{vy} = M_o\left(F_{vx}\right) + M_o\left(F_{vz}\right) = \int_{A_s} \tau_x(z - z_0)dS + \int_{A_s} \tau_z(x_0 - x)dS\,. \tag{7}$$

Where, p_x and p_z are weights of water pressure imposed by the ship on any surface in directions of x and z respectively; A_s is the ship surface; τ_x and τ_z are weights of viscous stress imposed by the ship on any surface in directions of x and z respectively; (x_0, y_0, z_0) is a centroid coordinate of the ship; (x, y, z) is a coordinate of any point on the ship surface.

Equation (8) can be established according to the force balance of the ship in the x-z plane, according to which longitudinal mooring force F_L of the ship, front transverse mooring force F_{T1} and back transverse mooring force F_{T2} can be calculated.

$$\begin{cases} \sum F_x = 0 \\ \sum F_z = 0 \\ \sum M_y = 0 \end{cases} \rightarrow \begin{cases} F_{px} + F_{vx} + F_L = 0 \\ F_{pz} + F_{vz} + F_{T1} + F_{T2} = 0 \\ F_{T1}\left(x_0 - x_1\right) + F_{T2}\left(x_0 - x_2\right) + M_{py} + M_{vy} = 0 \end{cases} \tag{8}$$

In the course of water conveyance in the lock chamber, as the water rises, the ship is subject to variable accelerated motion along the vertical direction. The motion equation of the ship is constructed according to Newton's second law of motion.

$$\begin{cases} F_{py} + F_{vy} - m_s g = m_s v\left(t\right), \\ F_{py} = \int_{A_s} p_y dS, F_{vy} = \int_{A_s} \tau_y dS. \end{cases} \tag{9}$$

Where, F_{py} and F_{vy} are weights of water pressure and viscous force in y direction respectively; m_s is the ship quality; g is acceleration of gravity; $v(t)$ is motion velocity of the ship at the moment t; p_y and τ_y are weights of water pressure and viscous force of the ship on any surface in y direction respectively; the remaining symbols are the same as above.

2.3. Three-dimensional numerical model

This Thesis is based on the water conveyance system of ports at side of long gallery at the bottom of lock with lock size as 170m×23m×3.5m (length× width ×the minimum water depth on the sill). With a 1000t single ship with basic dimen-

sion as 60m×10.8m×2.2m (length× width× minimum water depth) as the research object, a geometric ship and a overall three-dimensional mathematical model of the lock chamber is established and divided with grids with GAMBIT software. As for numerical simulation of water conveyance process in the lock chamber by using FLUENT software, there are three key problems to be solved. First, to improve the calculation accuracy, it is necessary to ensure the quality of the grid. In the pretreatment process, grids of the whole model are divided by zones, while since dynamic mesh models are used by ship motion and work valves, its surrounding area is divided and encrypted by using unstructured meshes, while structured girds are adopted for relatively structured areas, besides, surrounding areas of effluents from fracture surface of the port throat should also be encrypted. The ship grid and computational domain network are shown in Fig.3 and Fig. 4 respectively with initial position of the ship as central lock chamber. Second, it is about choice of numerical methods. In this Thesis, the control volume method is used to discretize the RNG $k \sim \varepsilon$ turbulence equation. The VOF model is used to track the free surface, while the wall boundary is treated by the wall-function method. The pressure and velocity coupling is solved by SIMPLEC algorithm. Third, it is about parallel computation of the ship's mooring force program. Due to the fact that special module to calculate stress process on the ship is not contained in FLUENT software, calculation of the ship's mooring force is realized by program interface UDF (User Defined Function) supplied by the software. There are three modules in the parallel calculation program, which are the calculation module of force process on the ship (Equation 5-9), the valve motion control module and the setting module for import boundary condition of calculation model. The most important part for this program is the coupling motion between the ship and water. In the course of the water conveyance in the lock chamber, due to the fact that the ship is subject to variable accelerated rectilinear motions, negative volume is likely to happen during grid reconstruction due to too fast motion speed of the ship, thereby affecting smooth calculation. Therefore, in the programming and debugging process, motion speed of the ship and water flow force along its movement direction are subject to homogenization treatment, which means that the total computing time is divided into a plurality of movement periods and the ship is moving at a constant speed in each period, that speed of the current period is the sum of speed value in the last time period and speed change value after time average treatment. 20 calculation steps are regarded as a movement period in the Thesis.

Fig. 3. Ship grid

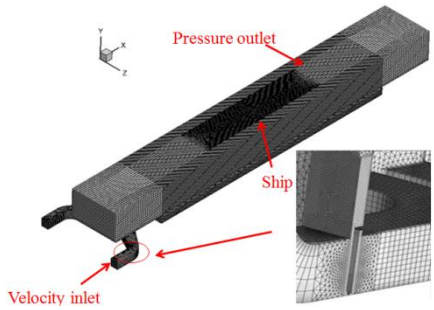

Fig. 4. Computational domain grid

3. Physical model tests

The physical model test carried out in this Thesis is used to verify rationality and correctness of the mathematical model. According to the selected water conveyance system of port at side of long gallery at the bottom of lock, based on lock scale (170m * 23m * 3.5m), it is assumed that fracture surface of gallery in the work valve section is 2×3.5m×3.5m=24.5m2, fracture surface of the main gallery is 2×2.6m×5.0m =26.0m2, port space is 0.22×23m =5m and ratio of total area of fracture face of port throat and gallery area at the valve is 0.85. 24 outlet ports which are set at each side of outlet section of the gallery at the bottom of lock, are arranged along the water flow direction on fracture surface of the port throat with three groups (8 ports each group) divided with port mouth sizes as 0.85m×0.9m, 0.75m×0.9m and 0.65m×0.9m separately for each group and overall size of outlet ports as 32.4m2.

The general layout of the physical model is shown in Fig. 5. The whole model which is designed according to the gravity similarity principle with scale as 1:25, valve working head as 15.7m, water filling time as 9min and total length as 10m, includes a upstream reservoir, a upstream approach channel, a water conveyance system, a lock chamber, a ship and a lifting baffle. The upper guide navigation channel is controlled by overflow type flat water tank; the water conveyance valve is controlled by stepper motor driven hoist with stepless speed regulation; the resistance-type pressure sensor is used to determine change of water level in the lock chamber. The ship's mooring force in the lock chamber is measured with the whole loop resistance testing device containing a longitudinal force ring, a front (back) transverse force ring, a rectangular steel ring and a contact roller developed by Nanjing Hydraulic Research Institute. The testing device for the ship's mooring force is shown in Fig. 6.

3.1. Water level in the lock chamber and ship displacement verification

Comparison diagram of measured water level value during water conveyance in the lock chamber and calculation value of the numerical model is shown in Fig. 7.

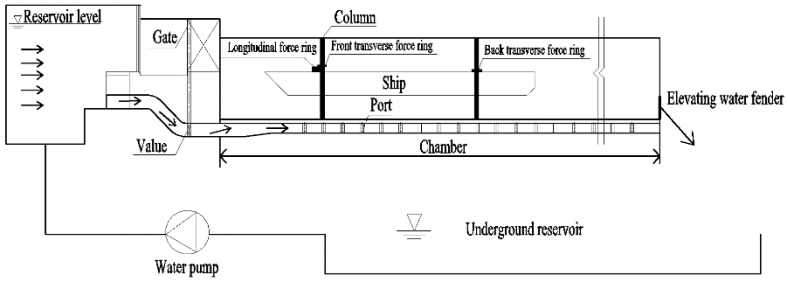

Fig. 5. General layout of physical model

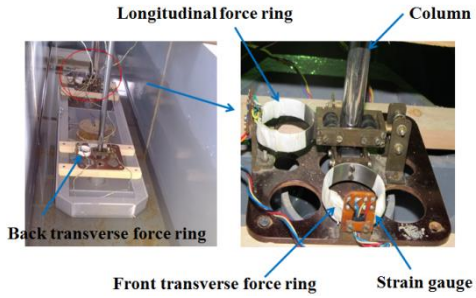

Fig. 6. Testing device for mooring force

It can be clearly found that the changing curve of water level in the lock chamber calculated according to numerical model is basically consistent with measured value of the model test with only 1% error, which indicates that the 3D mathematical model is able to simulate water conveyance process in the lock chamber. In this process, in virtue of coupling function between the ship and water flow, motion process of the ship is not synchronous with rising water level in the lock chamber from micro aspect and is considered as near synchronization from macro aspect. In the process of testing the ship's mooring force, the changing process of water level in the lock chamber is also recorded. Comparison diagram of water level in the lock chamber and ship displacement is shown in Fig. 8, which shows relatively good matching and parallel state of the two curves, which indicates basis synchronization between rising process of the ship and changing water level in the lock chamber, which is consistent with the actual lockage process of the ship, for which the ship's motion control equation proposed in this Thesis is reasonable.

3.2. Verification on Mooring Force of the Ship

It is found from the physical model test that transverse mooring force of the ship is sensitive to changes of flow function, that it is difficult to compare figures due to alternate appearance of peaks and valleys within a short period of time, that it will be difficult to find rules due to smaller values, for which measured values of longitudinal mooring force of the ship are compared with the calculated values, as shown in Figure 9 with the horizontal axis representing water conveyance time

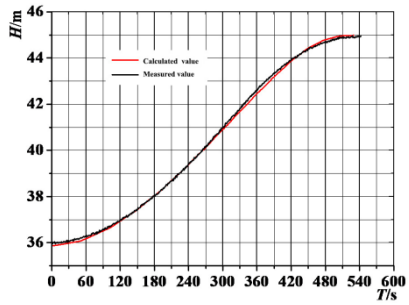

Fig. 7. Comparison between measured value and calculated value of water level in the lock chamber

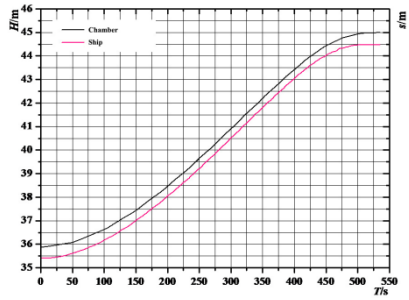

Fig. 8. Comparison between water level in the lock chamber and ship displacement

and the vertical axis representing magnitude of longitudinal mooring force. It is important to note that unapparent change of longitudinal mooring force is showed due to gradually steady water level in the lock chamber in middle and late period of water conveyance in the lock, for which comparison between measured values and calculated values of longitudinal mooring force in first 200s only is shown in Fig. 9. It can be clearly seen from the diagram that the calculated values of the mathematical model are basically consistent with the measured values, that all of them go through four oscillation periods and that the cycles decrease in turn. In the first 100s, the trend of the two process curves is almost the same. The first wave trough appears at the time of T=20s with measured value as -4.0kN, the calculated value as -4.2kN, and the error as 5%. In 100s-200s, certain staggering peaks appear in the two curves, but there is only little difference for value size. The measured and calculated values of longitudinal mooring force at each characteristic moment are shown in Table 1. The analysis shows that the parallel calculation program, which is reasonable for calculation of ship mooring force and has high accuracy, can reflect berthing conditions of the ship effectively.

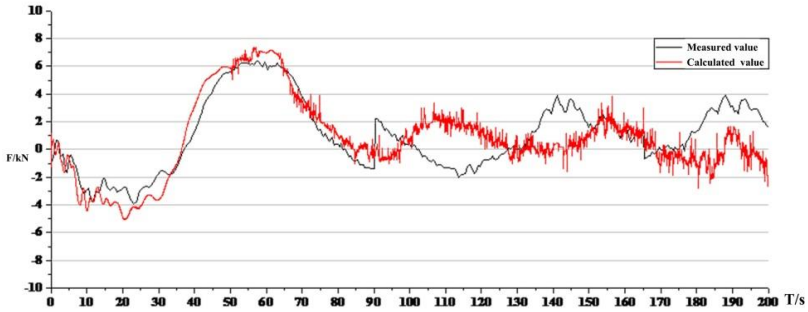

Fig. 9. Comparison between measured values and calculated values of the ship's longitudinal mooring force

Table 1. Measured values and calculated values of longitudinal mooring force at characteristic moments

Mooring force (kN)	T=20s	T=60s	T=90s	T=115s	T=145s	T=170s	T=190s
Measured value	-4.0	6.2	-1.7	-1.9	2.6	-0.2	2.3
Calculated value	-4.2	6.6	-1.6	1.1	-1.8	-0.4	1.8

4. Results analysis

Single variable method which means the constant—overall area of fracture surface of the port throat is used to analyze principles of influence of aspect ratio (λ=w/h) and number (δ) on hydraulic characteristics of the lock and the ship's mooring force. It can be learnt from the model test that gentle outflow of ports, steady rise of water level in the lock chamber and weakening function of wave & local forces are observed in the late period of water conveyance, that relatively lower starting water level is observed in the initial period of water conveyance, that with water flowing in the lock chamber, inclined water surface is caused, which triggers periodic long-wave movement, for which multiple superposition of the forward wave and the reflected wave, disordered flow state and obvious change of mooring force caused by complicated water flow function on the ship are observed, thereby it is easy to compare and select many schemes. In the meantime, due to the limitation of computer operation resources, the numerical simulation only calculates the initial stage of water conveyance. Calculation of working condition is shown in Table 2.

Table 2. Calculation of working condition

Factor	No.	Port's fracture surface (w×h×No.)	Value
λ	1	0.65×1.05×48	0.62
	2	0. 85×0.80×48	1.06
	3	1.13×0.60×48	1.88
	4	1.36×0.50×48	2.72
δ	5	1×0.9×36	36
	6	0.85×0.80×48	48
	7	0.75×0.72×60	60

4.1. Calculation of the ship's mooring force corresponding to different λ values

With total area of fracture surface of port throat and port number remained as constants, λ which changes in (0.62-2.72) interval, covers all aspect ratios of ports in actual lock works. The ship's mooring force in the lock and flow characteristics under various conditions are calculated and analyzed through numerical simulation on water conveyance process in the lock chamber by using FLUENT software. When λ changes, process curve for change of mooring force under various conditions is obtained through parallel calculation program on the ship's mooring force. The calculation curve for longitudinal mooring force under various work conditions is as shown in Fig. 10 (a), while calculation curves for front & back transverse mooring force are shown in (b) and (c) separately. According to (a), the trend of the four longitudinal force curves is basically the same, but with increase of water conveyance time, especially after 115s, working conditions 1 and 3 are subject to strong fluctuations with suddenly increase of longitudinal mooring force. For example, longitudinal forces of working condition 1 and 3 are -6kN and -3kN separately at the time of 130s, while longitudinal forces of working condition 2 and 4 are -1.1kN and -1.8kN respectively, which are far less than the preceding two working conditions. It can be learn from analysis of (b) and (c) that transverse force curve of working conditions 1 and 3 are subject to serious oscillation after 115s, that their transverse forces reach the maximum value as -12kN and -16kN respectively at the time of 150s. It indicates that uneven outflow from ports and stronger function of complicated water flow on the ship show with aspect ratios as 0.62 and 1.88 used, which has adverse affects on ship safety. Calculation values of the ship's mooring force under working conditions 1-4 at the time of T=115s are shown in Table 3.

Table 3. Calculation values of the ship's mooring force under working conditions 1-4 at the time of T=115s

No.	Longitudinal force (kN)	Front transverse force (kN)	Back transverse force (kN)
1	-2.2	-5.9	-2.0
2	-0.2	-0.5	-0.7
3	-3.8	-1.4	-1.6
4	-0.3	-0.9	-1.1

4.2. Flow characteristics in the lock chamber corresponding to different λ values

At the characteristic time of T=115s, X=30m, 60m and 90m fracture surface is taken along the longitudinal direction of the lock chamber, which correspond to front, middle and back positions of the ship, based on which flow velocity distribution of each fracture surface is analyzed; Y=0.5m, 4.5m and water surface of the lock chamber are taken along the vertical direction of the lock chamber, which corresponding to horizontal section of the port throat, horizontal section of turbulent fluctuation area at the bottom of the ship, based on which flow velocity distribution of horizontal section is analyzed. For limited length, only the most important veloc-

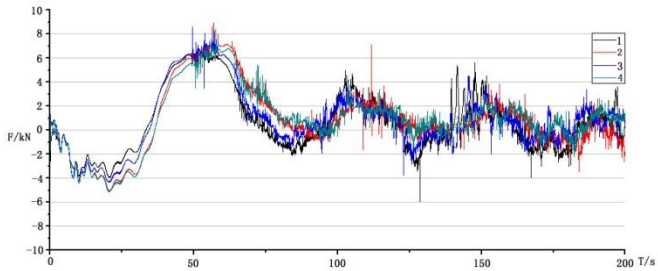

(a) Longitudinal force

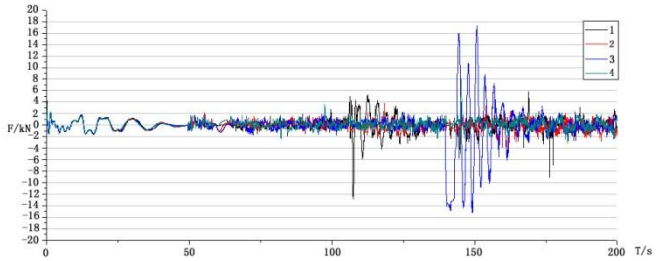

(b) Front transverse force

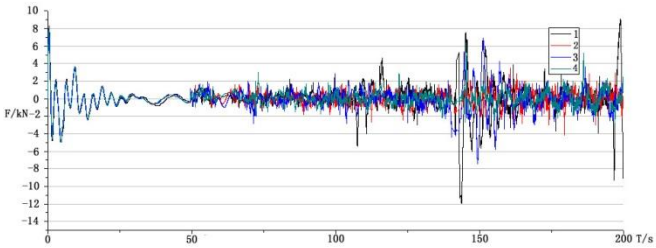

(c) Back transverse force

Fig. 10. The ship's mooring force under working conditions 1-4: (a) Longitudinal force; (b) Front transverse force; (c) Back transverse force

ity distribution at Y=4.5m (Fig. 11) is enumerated in this Thesis. The remaining calculation results are listed in Table 4.

Table 4. Mean velocity of each fracture surface at the time of T=115s under working conditions 1-4

No.	Transverse section (X, m/s)			Horizontal section (Y, m/s)		
	30m	60m	90m	0.5m	4.5m	Water level in the lock chamber
1	1.5	0.8	1.0	6.0	0.5	0.9
2	1.0	0.6	0.6	6.5	0.4	0.7
3	1.4	0.7	1.0	6.0	0.6	0.8
4	1.5	0.8	1.0	6.5	0.5	0.9

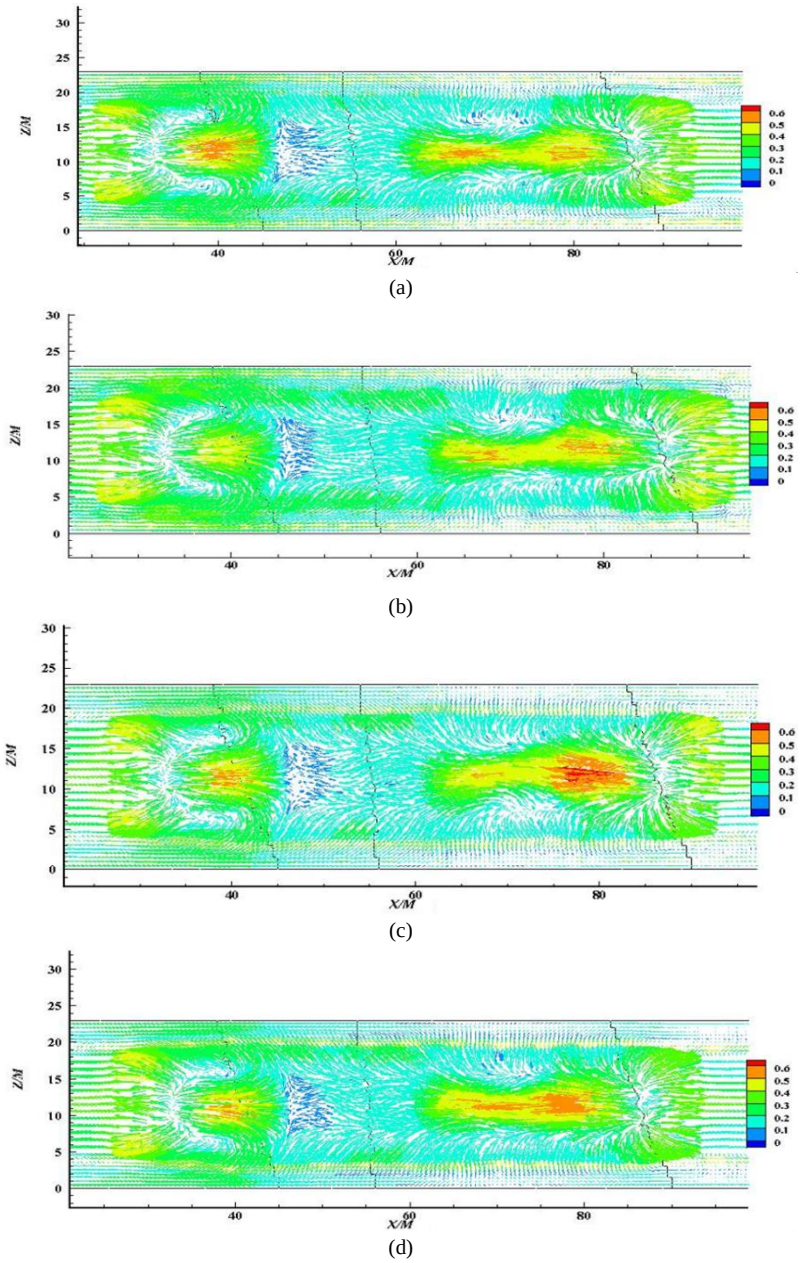

Fig. 11. Flow velocity distribution of horizontal plane in the lock chamber at the time of Y=4.5m under different λ layouts; (a) Working condition 1; (b) Working condition 2; (c) Working condition 3; (d) Working condition 4.

It can be learnt from analysis of data in Table 4 that when a change to λ occurs, the mean flow rate of each cross section under working condition is less than the

other conditions, which indicates that force of water flow on front, middle and back parts of the ship is relatively event and bumps and waggles resulted therefrom is relatively slight. At the same time, when layout under working condition 2 is used, flow rate of turbulent fluctuation area at the bottom of the ship and flow rate at water surface of lock chamber are 0.4m/s and 0.7m/s separately, which indicates that when λ approaches 1, degree of concentration of outflow from a single port is relatively scattered, energy dissipation by collision of water flow is sufficient, impact function of remaining energy of water flow at the bottom of the ship is decreased and the berthing condition is the optimal condition. Quantization of the ship's berthing condition is directly reflected in Fig. 9 and Table 3. It is not difficult to find that the mooring force under the working condition 2 is the smallest with smooth curve trend is smooth and free of zigzag fluctuation in good symmetry and stable amplitude of variation. In conclusion, it is not appropriate to choose aspect ratio of fracture surface of the port throat of scattered water conveyance type for the lock near 0.5 and 2, while when the value is between 0.9-1.1, the good outflow effect and the lock's berth condition can be obtained.

4.3. Calculation of the ship's mooring force corresponding to different δ values

Based on the research results of λ, with overall outflow area of fracture surface of the port throat as an constant, three different working conditions—1×0.9(λ=1.11, δ=36),0.85×0.80(λ=1.06, δ=48), 0.75×0.72(λ=1.04,δ=60) are selected for fracture surface to carry out research on number of ports. Figures 12 (a), (b) and (c) denote the longitudinal mooring force, the front and the back transverse mooring forces under working condition 5-7 respectively. It can be seen from the diagram that when the number of ports changes, that the mooring force of the ship changes little and that the trend of the three curves is basically consistent. The longitudinal and transverse mooring forces in small scope increase slightly at the time of T=140s under the working condition 6. But on the whole, unstable changes under each water conveyance period, sudden increase or decrease at many points of the curves and relatively poor symmetry are observed under working conditions 5 and 7, and the two curves fluctuate violently at the time of T=50s, 100s and 150s, which indicates relatively strong swing of the ship in the lock chamber, based on which it can be inferred that working conditions 5 and 7 are not optimal layouts. Calculated values of mooring force at the time of T=115s under working conditions 5-7 are as shown in Table 5.

Table 5. Calculation values of the ship's mooring force at the time of T=115s under working conditions 5-7

No.	Longitudinal force (kN)	Front transverse force (kN)	Back transverse force(kN)
5	-1.4	-1.5	-2.6
6	-0.6	-2.2	-1.8
7	-1.2	-2.4	-3.7

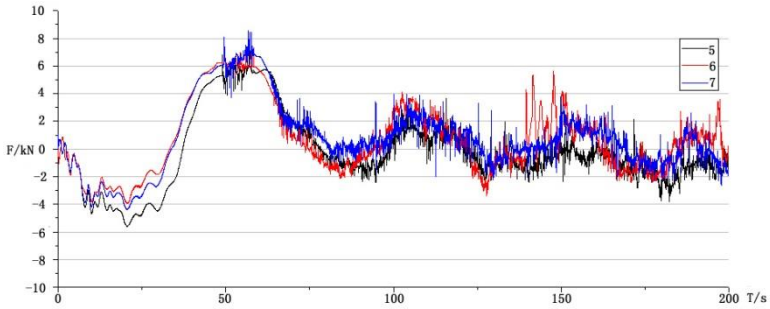

(a) Longitudinal force

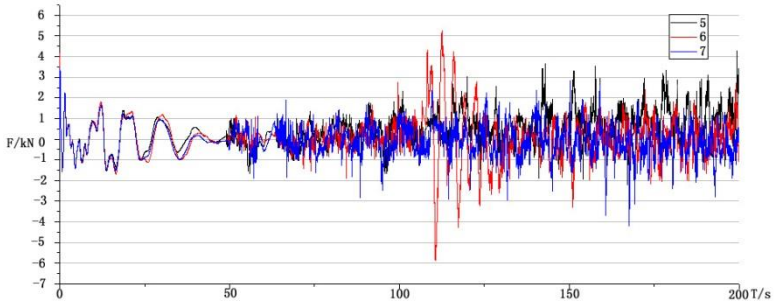

(b) Front transverse force

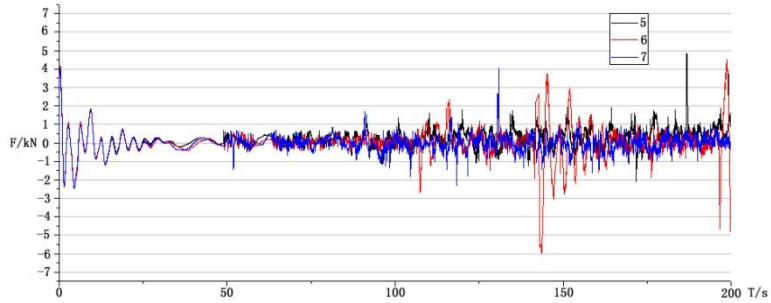

(c) Back transverse force

Fig. 12. The ship's mooring force under working conditions 5-7; (a) Longitudinal force; (b) Front transverse force; (c) Back transverse force.

4.4. Flow characteristics in lock chamber corresponding to different δ values

Selection of fracture surface is identical to choice under working conditions 1-4; therefore, discussion is not required. Flow rate distribution of horizontal section of the lock chamber at the time of Y=4.5m under different δ layouts is shown in Fig. 13 with average flow rate on each fracture surface summarized in Table 6.

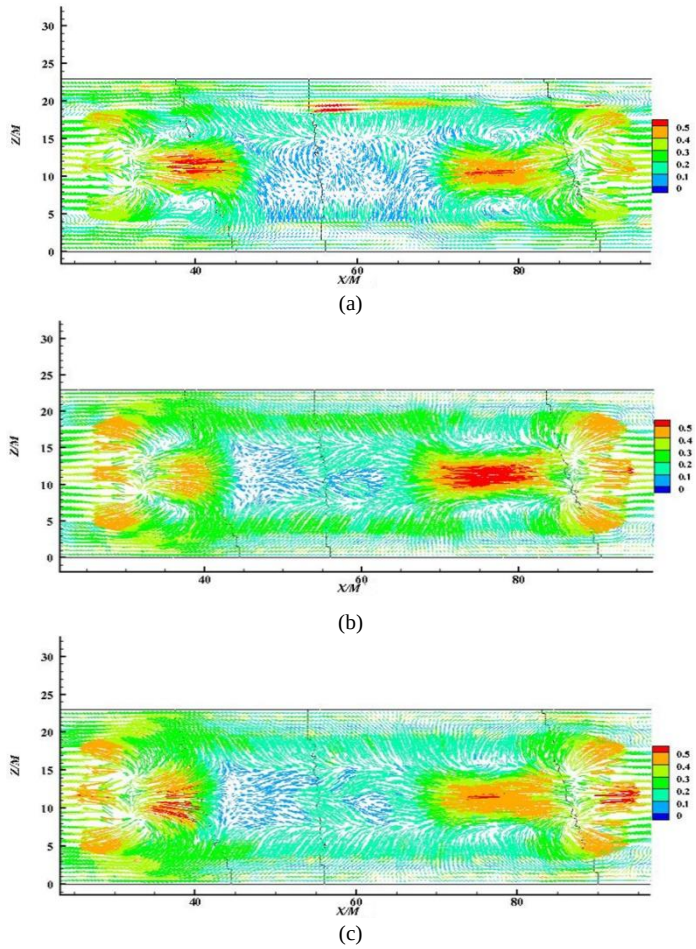

Fig. 13. Flow rate distribution of horizontal section of the lock chamber at the time of Y=4.5m under different Δ Layouts; (a) Working condition 5; (b) Working condition 6; (c) Working condition 7.

Table 6. Average flow rate on each fracture surface at the time of T=115s under working conditions 5-7

No.	Transverse section (X, m/s)			Horizontal section (Y, m/s)		
	30m	60m	90m	0.5m	4.5m	Water surface of the lock chamber
5	2	1.0	2	5.5	0.5	0.8
6	1.6	1.0	1.5	6	0.3	0.5
7	1.9	1.0	1.6	5.5	0.4	0.7

According to calculation results of the ship's mooring force in Fig. 12 and Table 5, it can be found that when overall area of fracture surface of the port throat and aspect ratio are the same, changing number of ports has relatively little total

influence on the ship's mooring force. But it can be seen through the analysis of detailed features of stress process line that too many or too few ports will cause unstable mooring forces during the characteristic water conveyance period and relatively poor berthing condition for the ship. It can be learned from calculation results of water flow characteristics that there are relatively large flow rate at the bow and stern regions and relatively small flow rate at the middle of the ship under layouts of working conditions 5 and 7, which indicates that too many or too few ports will reduce uniformity of the water body in the lock chamber, resulting in uneven stress distribution of the ship as a whole, further explaining reasons for fluctuation of the mooring force curve. The flow rate distribution in horizontal turbulent fluctuation area at the bottom of the ship is shown in Fig. 13. Turbulent kinetic energy is not evenly distributed at the bow and the stern with values at the stern lager than values at the bow under working conditions 5 and 7. Flow rate of water surface in the lock chamber under working condition 6 is 0.5m/s which is less than values under the other two working conditions, besides, its turbulent kinetic energy at the stern is slightly later, but it has relatively good overall symmetry, which indicates that δ under working condition 6 relatively approaches the optimal value. Therefore, in the design of dispersive water conveyance type of the lock, number of ports should be 2-2.2 times of the lock's width, and the specific value still needs to be determined according to working heads of the lock, gallery length, construction difficulty, construction cost and other aspects.

5. Conclusion

The following conclusions can be drawn by using FLUENT computing platform for large fluid mechanics in this Thesis, through the establishment of overall 3D mathematical model of water conveyance system of ports at side of long gallery at the bottom of lock, based on comprehensive research on different aspect ratios of fracture surface of the port throat and number of ports in the lock manifold system and comprehensive comparison & analysis of the ship's mooring forces and hydraulic characteristics under different working conditions:

(1) The ship's longitudinal & horizontal forces and motion control equation is established based on dynamic response of fluid-structure interaction, besides, UDF functions of the software are used to write parallel calculation program for the ship's mooring force, achieving secondary development of FLUENT software. After verification of the physical model test, the numerical method is proven reasonable and feasible and satisfies relatively high accuracy requirements on the whole; therefore, it can be used for further research on the ship's mooring force.

(2) Different aspect ratios (λ) show that when value around 0.5 and 2 is take by λ, flow rates on fracture surfaces at front, middle and back parts of the ship are not distributed evenly with relatively large longitudinal scope, while mooring forces increase sharply with extension of water conveyance time. When λ is close to 1, minimum mooring force of the ship appears with stable change, reducing concentration degree of outflow from a single port, which leads to even distribution of water flow in the lock chamber. Energy dissipation collided by outflow of the ports is relatively

sufficient when flow rate on the stern area is 0.4m/s. Therefore, when λ value is in the 0.9-1.1 interval, the berthing condition of the ship is better.

(3) Number of ports (δ) is closely related with the chamber width. When δ changes, trend of the ship's mooring force curves under working conditions 5, 6 and 7 is basically consistent. But on the whole, there are relatively obvious fluctuations during typical water conveyance period under working conditions 5 and 7, which is not conducive to the ship safety. Though there are a little oscillation at the time of T=150s in the process line under the working condition 6, the duration is short and it is smooth in general with stable performance, which indicates that δ under working condition 6 is located in a reasonable range but still needs to be further optimized. Combined with hydraulic characteristics of the lock chamber at the characteristic moment, flow rates of water surface in the lock chamber under working conditions 5 and 7 are 0.8m/s and 0.7m/s separately, which are larger than 0.5m/s. besides, uneven distribution of flow rate on each part of the ship indicates relatively weak energy dissipation effects of too many or too few ports, resulting in reduced uniformity of water body in the lock chamber and easily leading to swing up and down of the ship. Therefore, it is suitable for δ as 2-2.1 times of chamber width, under which condition relatively good flow condition can be obtained in the lock chamber.

Acknowledgement

The National Natural Science Foundation of China (Grant no. 51509027); the Foundation of Chongqing Municipal Commission of Education of China (Grant no. KJ1400322); the Foundation of Scientific Innovation of Chongqing Graduates of China (Grant no.CYB15112).

References

[1] Y. Y. Zhang, Q. Li, W. J. Welsh, P. V. Moghe, and K. E. Uhrich: *Micellar and Structural Stability of Nanoscale Amphiphilic Polymers: Implications for Anti-atherosclerotic Bioactivity*, Biomaterials, *84* (2016), 230–240.

[2] J. W. Chan, Y. Y. Zhang, and K. E. Uhrich: *Amphiphilic Macromolecule Self-Assembled Monolayers Suppress Smooth Muscle Cell Proliferation*, Bioconjugate Chemistry, *26* (2015), No. 7, 1359–1369.

[3] D. S. Abdelhamid, Y. Y. Zhang, D. R. Lewis, P. V. Moghe, W. J. Welsh, and K. E. Uhrich: *Tartaric Acid-based Amphiphilic Macromolecules with Ether Linkages Exhibit Enhanced Repression of Oxidized Low Density Lipoprotein Uptake*, Biomaterials, *53* (2015), 32–39.

[4] Y. Y. Zhang, A. Algburi, N. Wang, V. Kholodovych, D. O. Oh, M. Chikindas, and K. E. Uhrich: *Self-assembled Cationic Amphiphiles as Antimicrobial Peptides Mimics: Role of Hydrophobicity, Linkage Type, and Assembly State*, Nanomedicine: Nanotechnology, Biology and Medicine, *13* (2017), No. 2, 343–352.

[5] M. A. Arie, A. H. Shooshtari, S. V. Dessiatoun, et al.: *Numerical modeling and thermal optimization of a single-phase flow manifold-microchannel plate heat exchanger*[J]. International Journal of Heat & Mass Transfer, *81* (2015), 478–489.

[6] Zhang C., Zhang J. F., Feng P. F., et al.: *Research on Modeling and Optimiza-*

tion of a Dual Chamber Air Spring Vibration Isolation System[J]. Advanced Materials Research, *702* (2013), 310–317.

[7] J. Yu, J. F. Feng: *Experimental Research on the Parameter Optimization of a Radiant Floor Heating System with Reflective Modules*[J]. Applied Mechanics & Materials, *353-356* (2013), No. 353-356, 3114–3119.

[8] L. Bingjie, Z. Jiahong, W. Xu W., et al.: *Research on Air Flow Measurement and Optimization of Control Algorithm in Air Disinfection System*[J]. Measurement Science Review, *13* (2013), No. 1, 39–44.

[9] L. He, Z. Li, Z. Guo: *Research on Hydraulic Manifold Block Hole Routing Optimization Based on Improved Ant Colony Algorithm*[C]// International Conference on Advances in Mechanical Engineering and Industrial Informatics (2015).

[10] Y. Wang, M. Duan, J. Feng J., et al.: *Modeling for the optimization of layout scenarios of cluster manifolds with pipeline end manifolds*[J]. Applied Ocean Research, *46* (2014), No. 3, 94–103.

[11] X. Zhang, X. Fu X., X. Yuan X.: *Simulation Based Parallel Genetic Algorithm to the Lockage Co-scheduling of the Three Gorges Project*[C]// International Conference on Computer Science and Software Engineering. IEEE, (2008), 324–327.

[12] H. Schättler: *Regularity properties of time-optimal trajectories of an analytic single-input control-linear system in dimension three*[J]. Journal of Optimization Theory & Applications, *59* (1988), No. 1, 135–146.

[13] S. Krishnan, P. Y. Lee, J. B. Moore, et al.: *Global registration of multiple 3D point sets via optimization on a manifold: US*, US 7831090 B1[P] (2010).

[14] D. H. Lee, J. M. Oh, H. Y. Jeong, et al.: *Spray Behavior Characteristics of Injector Used for HC-DeNOx Catalyst System in the Transparent Exhaust Manifold*[J]. Transactions of the Korean Society of Automotive Engineers, *15* (2007), No. 4, 54–60.

Received May 7, 2017